Control of vortex chirality and polarity in magnetic nanodots with broken rotational symmetry

V. Cambel[1,*] and G. Karapetrov[1,2]

[1]*Institute of Electrical Engineering, Slovak Academy of Sciences, Dúbravská cesta 9, SK-841 04 Bratislava, Slovakia*
[2]*Department of Physics, Drexel University, 3141 Chestnut Street, Philadelphia, Pennsylvania 19104, USA*

We explore size-dependent magnetic states of sub-100-nm Permalloy nanomagnets. The geometry is suitable for independent setting and readout of vortex polarity and chirality by applying in-plane magnetic fields only. Micromagnetic calculations show that in "Pac-Man"-like magnetic nanodots the relaxation channels to specific chirality and polarity states from uniform magnetization state are deterministic and are not influenced by the presence of moderate out-of-plane fields. The particular geometry opens a straight channel for magnetization relaxation toward a stable closure-domain vortex state with specific chirality and polarity. We show that in these nanomagnets the write process is simple and the signal is easily readable.

Recent developments in controlled manipulation of magnetic domains in ferromagnet nanostructures have opened opportunities for unique memory architectures that have higher storage density, faster performance, and require lower power to write and read the information. Increasing the energy efficiency of such devices is of paramount importance, and breakthroughs in this area will have an immediate impact on overall energy consumption.[1] The power consumption parameter can outweigh seemingly important features such as scalability and reliability, as in the example of the racetrack memory architecture.[2] It is certain that any prospective magnetic memory architecture has to have a well-defined switching field, narrow switching field distributions for large numbers of elements, and a reproducible switching behavior.

In this paper we study the properties of a nonvolatile magnetic memory element with broken rotational symmetry. The intriguing property of this sub-100-nm magnetic structure is in its ability to store two bits of information simultaneously (in terms of chirality and polarity of the magnetic vortex), and each bit can be addressed by application of an in-plane magnetic field only. The proposed nanoscale magnetic memory element has a highly stable fourfold degenerate remanent state at room temperature and both chirality and polarity can be read using conventional magnetic readout schemes. Below we describe in detail the idea behind the chosen geometrical structure, the results of the micromagnetic simulations of the magnetization states of the element, the switching mechanism between the four magnetic ground states, and we explore the magnetic phase diagram of the remanent state of the nanomagnet.

The magnetic vortex ground state exists in a wide range of nanodot sizes.[3] The vortex state is characterized by two topological quantities: polarity, which is the magnetization direction of the vortex core, and chirality, which is the rotational direction of the in-plane magnetic moment. These two quantities are independent in circularly symmetric nanodots and therefore they can be used to store and read two bits of information, resulting in four different states of the magnetic nanodot. There are two main problems in the application of a perfectly symmetric circular nanostructure as a magnetic memory element: First, it is difficult to read and set the vortex chirality since there are no stray magnetic fields emanating from such a spin structure,[4,5] and second, it is necessary to apply an out-of-plane magnetic field in order to set the vortex

core polarity.[6–9] Attempts to address the first issue have led to the use of odd-symmetry structures (triangles, pentagons) in which it is possible to define and, to a certain extent, to read the chirality of the vortex state in these nanoelements[5,10] that have gaps in their circular closure state.[11] The second issue has been addressed by applying time-dependent in-plane and/or circularly rotating in-plane fields in order to change the remanent state on the nanomagnet.[6,12–14]

In this paper we study the magnetic properties of nanomagnets with sub-100-nm lateral dimensions, one order of magnitude smaller than those studied in Refs. 4, 5, and 10. These structures have a potential of producing storage densities close to 1 Tbit/in.[2]. Based on micromagnetic calculations, we have designed a "Pac-man"-like (PL) nanomagnet, and calculated its magnetic properties, showing how to control its polarity and chirality by applying in-plane fields only.

In the calculations we have used the OOMMF code,[15] which solves the micromagnetic problem using the Landau-Lifshitz-Gilbert equation. The parameters used for Permalloy (Py) are as follows: saturation magnetization $M_s = 8.6 \times 10^5$ (A/m), exchange stiffness $A = 1.3 \times 10^5$ (J/m), without any crystalline anisotropy, and a damping coefficient equal to 0.5. The cell size was 1 nm, except where noted explicitly, and this value is much smaller than the magnetic exchange length in the real material ($l_m = \sqrt{\frac{2A}{M_s^2}} \sim 5.5$ nm). It is well established that exchange interaction dominates in smaller magnetic particles, resulting in a single domain state.[16] As the size of the magnetic structure increases, the magnetostatic interaction becomes relevant and multidomain states are formed. In circular planar disks the transition from a single domain state to a magnetic vortex state takes place as the disk lateral size is increased. In smaller disks the exchange energy suppresses vortex nucleation and therefore the remanent state with a vortex core cannot be reached as easily as in larger disks.[3] In this region of metastability, single domain and vortex states correspond to two distinct minima separated by an energy barrier. The energy barrier between the two metastable states prevents the transition to the lowest-energy state.[17] In order to suppress the barrier to reaching the vortex state from a uniform in-plane magnetization state, we chose a circular object with broken rotational symmetry, i.e., a "Pac-man"-like nanomagnet. Our nanostructure geometry is conceptually different from

previous investigations of the magnetic properties in Pac-man shaped magnets.[18]

Our PL nanostructure is composed of a central disk and the outer ring with a missing sector, which is reminiscent of a horseshoe magnet. The central part is designed to hold the remanent vortex state, and the outer magnetic ring structure has two important purposes: to facilitate quick relaxation of the inner disk to a vortex state of designated polarity, and to enable easy readout of nanomagnet chirality (by measuring the in-plane magnetic field in the ring gap). In this paper we fixed the ratio of the inner to the outer diameters of the PL nanomagnet to 2/3 and the angular span of the missing segment to 45°, while we varied the outer diameter and the thickness of the structure.

In Fig. 1(a) we show nanodot size dependence of the total energy density of Py disks after relaxation from both uniform and vortex initial magnetization. The magnetic system *does not* transition between vortex and uniform magnetization states when it relaxes from either initial state. For the vortex remanent state, the role of the disk thickness is minor. Evidently, for disks larger than 100 nm, the absolute energy minimum is for the state with a vortex. On the other hand, an absolute energy minimum does not guarantee that the vortex is automatically

created in the disk due to a finite potential barrier between the uniform and vortex states.[17] Irregularities (or effectively a larger cell size in the simulation) would cause the disk magnetization to relax more easily from a local energy minimum to a remanent state with the lowest energy. From Fig. 1(a) we note that to achieve a vortex remanent state for a 50-nm-diam disk, its thickness must be above 40 nm, and the disk must have the possibility (open channel) to relax into a remanent state with a vortex. In the proposed PL geometry such a relaxation channel is open by design and a ground vortex state is always achieved for 40-nm thickness and diameters above 50 nm [Fig. 1(b)]. For PL structures of thicknesses 40 nm and more, the system always relaxes into a vortex state with the lowest energy. Instead, for thinner samples of the same diameter the remanent configuration is a single domain state with uniform in-plane magnetization. For a thickness value of 40 nm a crossover (first-order[19] or second-order[20] phase transition) from a Néel-type to a Bloch-type domain wall is observed in Py. A change in spin dynamic modes[20] below this thickness threshold is observed and it leads to a reduction of available channels for the system transition between uniform and vortex states. Below we describe the four degenerate remanent ground states of this system and the straightforward paths on how to reach each of them consistently. We will show how the geometry of the system coupled with the magnetic spin dynamics leads to a specific ground state of the nanomagnet.

The PL nanomagnet with a ring gap opening of 45° has a broken rotational symmetry. If vortex state magnetization is stabilized in this system, the chirality (in-plane spin magnetization direction) of the nanomagnet is determined by the magnetic history of the sample. If the remanent state is reached from a uniform state directed along the positive x axis, the chirality state will be counterclockwise due to asymmetry in the amount of local in-plane spins aligned parallel and antiparallel to the applied magnetic field. This purely geometrical effect caused by the cutout in the outer ring results in a lower magnetostatic energy of the system when the majority of the in-plane spins are aligned along the field. This is confirmed in micromagnetic calculations on the PL structure with an outer diameter of 70 nm and an inner diameter 2/3 of the outer one [Figs. 2(b) and 2(c)] with a thickness of 40 nm.
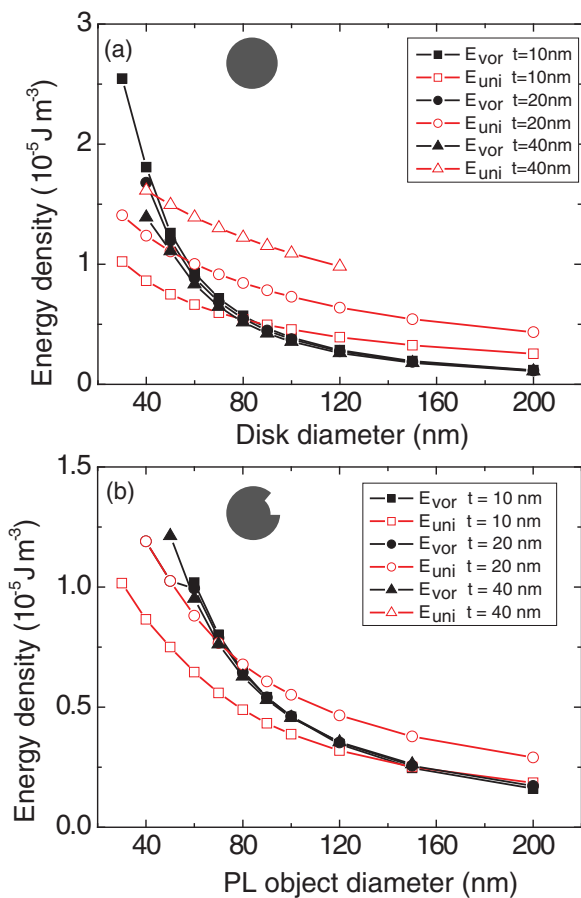

FIG. 1. (Color online) Energy density as a function of outer disk diameter for different disk thicknesses in case of disk-shaped (a) and "Pac-Man"-like (b) Permalloy nanodots. The final state energy densities are shown for two cases of uniform (open symbols) and vortex (closed symbols) initial magnetization.
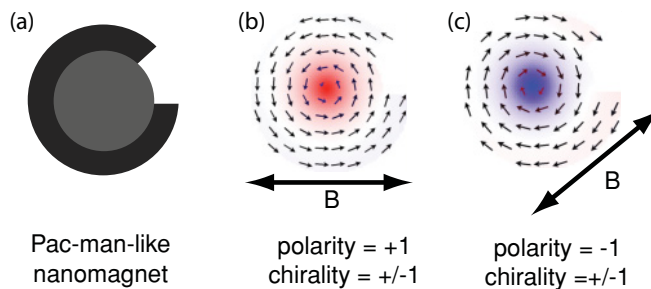

FIG. 2. (Color online) "Pac-Man"-like object (a) and its remanent state after relaxation from initial uniform magnetization along the $+x$ direction (b) and relaxation from initial uniform magnetization along the 45° direction (c). Sweeping the magnetic field in positive and negative directions changes chirality, but preserves the polarity of the vortex. The polarity of the vortex is changed by changing the angle of the applied magnetic field (along the x axis, negative vortex polarity; along 45°, positive polarity).

The application of a magnetic field along the positive x axis beyond the value needed to achieve uniform magnetization (saturation magnetization) with subsequent gradual reduction of the field to zero settles the system in a vortex state with counterclockwise chirality and positive polarity. A similar excursion of the field along 45° from the x axis in the positive direction results in clockwise chirality and negative polarity. Application of the field in the opposite direction in both cases leads to opposite chiralities, but the polarities remain the same.

Next, we focus on the nature of the vortex state of the PL nanomagnet, with particular emphasis on what determines the vortex polarity in the remanent state. Understanding the relaxation mechanism of the system from uniform in-plane magnetization to a vortex state would enable us to control the vortex polarization of the nanodot in the remanent state. We show that the vortex polarity can be deterministically set by application of an in-plane magnetic field only. The fascinating fact is that the desired vortex polarization can be obtained even in the presence of a small out-of-plane applied field component opposite to the desired vortex polarity. Micromagnetic simulations of the remanent state obtained from a uniformly magnetized state are shown in Figs. 2(b) and 2(c). The final remanent state of the PL nanomagnet is a vortex state with a large part of the magnetization oriented perpendicular to the plane of the disk ($M_z/M_s \sim 0.106$ for $d = 70$ nm). This is a consequence of a relatively small diameter of the PL object, which leads to a large relative contribution of the exchange energy. Another important factor is the thickness—40-nm-thick Py is already above the Néel-to-Bloch crossover point.[19,20] The vortex polarity in a PL nanomagnet in the remanent state is determined by the direction of the initial uniform polarization with respect to the cutout portion of the ring. If the applied magnetic field saturates the sample magnetization along the x axis, the final remanent state is with a positive vortex polarity. On the other hand, when the system relaxes from a uniform magnetization along 45°, the remanent state is with a negative vortex polarity. In both cases the vortex polarity does not depend on the sign of the magnetic field. To show the stability of the relaxation pathway to a particular state, an out-of-plane magnetic field of 10 mT in the direction opposite to the remanent vortex polarity is insufficient to cause a reversal of the polarity of the entering vortex during the transition to a remanent state for a PL with a diameter 70 nm. This shows that both vortex polarity and chirality in the PL nanomagnet can be deterministically set by application of in-plane fields only. The magnetic state of the PL can be read by measuring local out-of-plane and in-plane components of the magnetic field above the disk center and above the ring cutout, respectively. Therefore, the PL nanomagnet has four energetically equivalent ground states that can be accessed independently, and thus it could store two independent bits in one structure.

In order to determine the origin of the relaxation pathway into a predetermined ground state, we examined the magnetization curves of individual elements. The magnetization loops obtained from micromagnetic simulations are shown in Figs. 3(a) and 3(b). The transition from a uniform to a vortex state occurs at ±30 mT. On the other hand, the expulsion of the vortex from the PL nanomagnet occurs at ±120 mT. A closer inspection of the time evolution of the magnetization
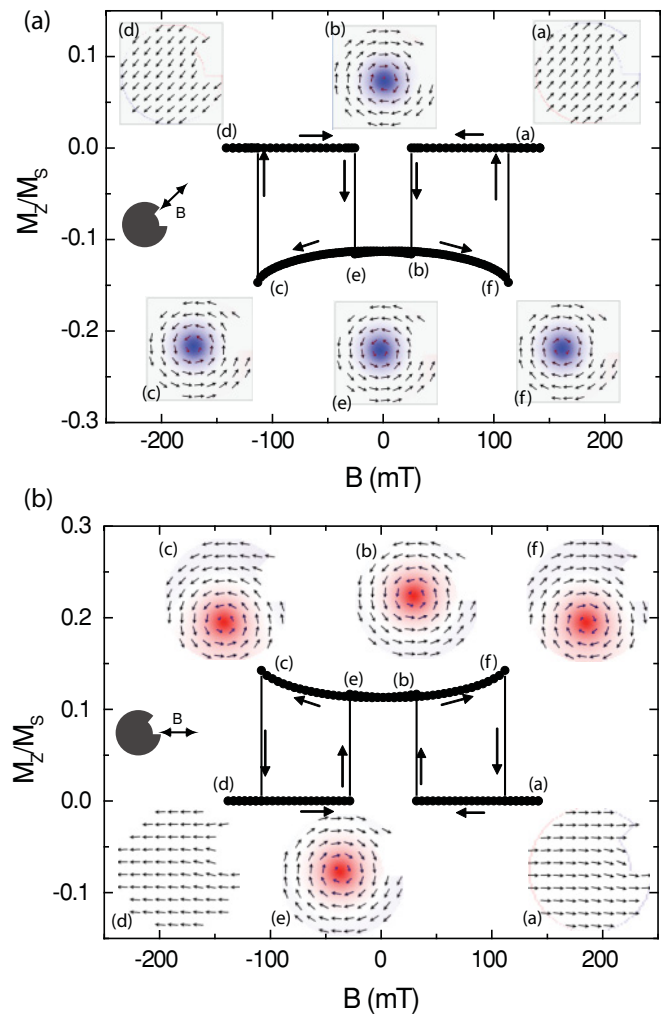

FIG. 3. (Color online) Hysteresis curve of a "Pac-Man"-like Py nanodot with an outer diameter of 70 nm, an inner diameter of 46 nm, and a thickness of 40 nm. The opening angle is 45° and the applied magnetic field is along the 45° direction. Magnetization states of the nanodot are shown at the following specific points in the hysteresis loop: +150 mT (a) → 0 mT (b) → −80 mT (c) → −150 mT (d) → 0 mT (e) → +80 mT (f), applied along 45° (upper panel) and along the x axis (lower panel). In the former case only negative polarity is achieved, with chirality determined by the magnetic history, while in the latter case only positive vortex polarity is present with each of chiralities.

process [Fig. 4(a)] shows that the vortex first enters the sample at the outer corner of the ring cutout that is not along the axis of the applied magnetic field. For example, if the initial uniform magnetization state is along the x axis, the vortex enters from the outer corner located at a 45° angle. On the other hand, the vortex exit always occurs from the lower part of the nanoparticle, as one would expect in the case of a circular disk of the same thickness and diameter. These pathways of vortex entry and exit hold true for disk thicknesses between 36 and 48 nm and outer diameters between 50 and 78 nm.

We examined the dependence of the vortex entry (B_{in}) and exit (B_{out}) fields on the size of the magnetic nanoparticle with a thickness fixed to 40 nm. The diameter dependence [Fig. 4(b)]
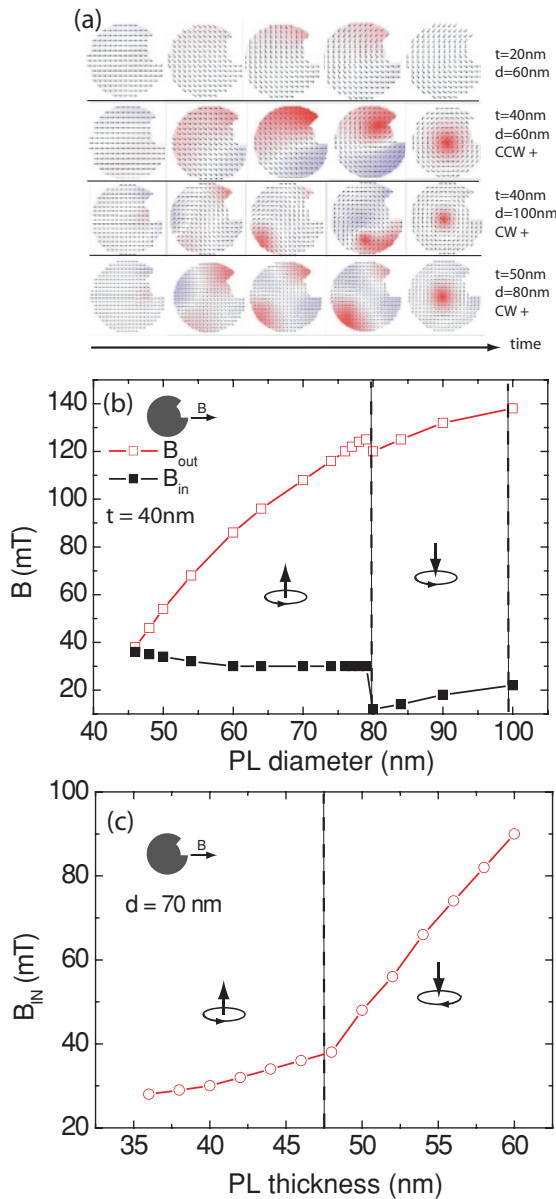
chirality also becomes unpredictable (i.e., sensitive to the field sweep rate, out-of plane field component) for larger diameter nanoparticles, which reflects the fact that the barriers between the four different final degenerate magnetic states diminish rapidly.

The thickness dependence of the vortex entry fields is shown in Fig. 4(c). The data is shown for thicknesses above 36 nm, since no vortex state is observed in thinner PL objects. In this figure we also see that the monotonous change in B_{in} has a kink at 48 nm. In this case we also have a very consistent relaxation into a predetermined state for thicknesses $36 < t < 48$ nm, and relaxation into different magnetic states for $t > 48$ nm, i.e., above the kink in the curve. A more detailed examination of the relaxation into remanent state from a uniformly magnetized state results in vortex phase diagrams, shown in Fig. 5. The diagrams describe the case when the magnetic field is applied along the $+x$ axis. Similar diagrams with opposite vortex polarities can be drawn for the case when the field is applied along $45°$, as discussed earlier. In the lower left-hand portion of the diagrams we have a stable region for which all four degenerate remanent magnetic states of the vortex can be set deterministically by applying in-plane magnetic fields only. The state is independent on the speed of magnetic field sweep

FIG. 4. (Color online) (a) Time evolution of a local magnetic domain structure from a full saturation state after removing the applied field abruptly in the case of different sizes of a PL nanomagnet. In the first case no vortex penetrates the structure due to small thickness. In the rest of the cases the vortex penetrates the PL structure at specific locations on the disk perimeter, setting up defined chirality of the vortex. The time scale necessary to achieve the equilibrium final state is ∼1 ns. (b) and (c) Vortex entrance (B_{in}) and exit (B_{out}) fields derived from magnetization loops for PL samples of different diameters (b) or thicknesses (c). The jump in curve (b) and the kink in curve (c) signal a transition to a different mode of vortex penetration into the PL nanomagnet, which sets up well-defined polarity and chirality of the vortex for the particular geometry.

shows a monotonous dependence, followed by a discontinuity in the B_{in} and B_{out} dependence at 80 nm. Closer examination of the magnetization process shows that for $d > 80$ nm the vortex entry has a topologically different trajectory from the case of $d < 80$ nm [Fig. 4(a)]. The final state of the vortex polarity and
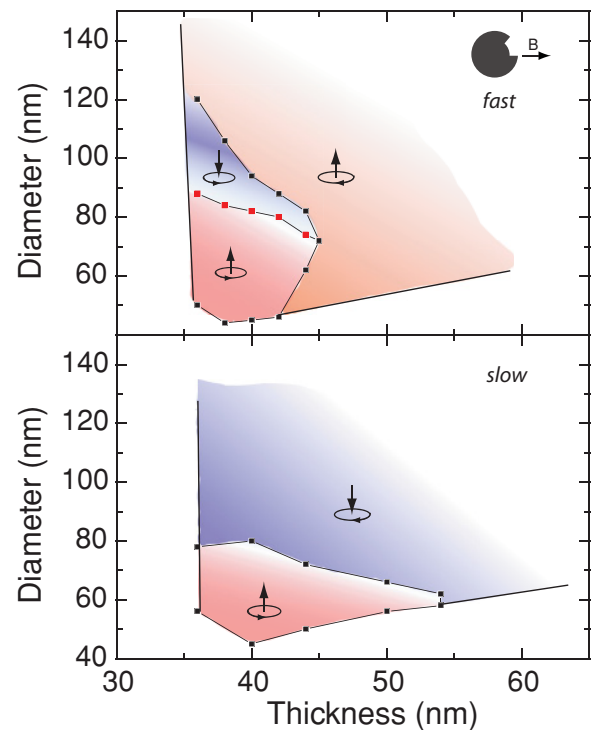

FIG. 5. (Color online) Phase diagrams of a remanent vortex state in a PL nanomagnet after saturation along the $+x$ axis. The remanent state is reached by immediately removing the applied field (fast—upper panel) or by equilibrating the magnetization at intermediate fields before reaching $H = 0$ (slow—lower panel). In the lower left-hand corner there is an area of stable remanent vortex configuration (red area) with a positive vortex polarity and counterclockwise chirality. The chirality will change to the opposite one across all the phase diagrams when applying a magnetic field along the $−x$ axis. Polarity, on the other hand, could be changed by saturating the PL nanomagnet along $45°$.

in this case. In the other portions of the diagram, not all of the states can be accessed, and the final state depends on how quickly the magnetic field is brought to zero.

It remains a challenge to experimentally confirm the findings from micromagnetic simulations due to the size of the PL structure. Scaling up the structure will completely change it magnetic behavior, and the polarity of the vortex state cannot be deterministically established using the same mechanism. At this point we foresee that synthesis of PL structures could be accomplished by scanning probe nanolithography or *e*-beam lithography with elaborate proximity corrections. The ultimate goal is to mass produce arrays of PL nanomagnets using nanoimprint lithography, which is a relatively cheap and scalable technique. Finally, we would like to point out that the results of the simulation are robust with respect to variations in the $45°$ angle of the "missing sector" of the PL structure. Similarly, the sharpness of the edges is not as important as the correct curvature of the inner circle (i.e.. "the belly") of the PL structure. The geometry of the inner circle is crucial for stabilizing the remanent vortex state and every effort should be made to properly fabricate this part of the PL structure.

---

[*]vladimir.cambel@savba.sk

[1]Mark Ellis, *Gadgets and Gigawatts: Policies for Energy Efficient Electronics* (OECD/IEA, Paris, 2009).

[2]S. S. P. Parkin, H. Hayashi, and L. Thomas, Science **320**, 190 (2008).

[3]S. H. Chung, R. D. McMichael, D. T. Pierce, and J. Unguris, Phys. Rev. B **81**, 024410 (2010).

[4]M. Schneider, H. Hoffmann, and J. Zweck, Appl. Phys. Lett. **79**, 3113 (2001).

[5]M. Jaafar, R. Yanes, D. Perez de Lara, O. Chubykalo-Fesenko, A. Asenjo, E. M. Gonzalez, J. V. Anguita, M. Vazquez, and J. L. Vicent, Phys. Rev. B **81**, 054439 (2010).

[6]B. Van Waeyenberge, A. Puzić, H. Stoll, K. W. Chou, T. Tyliszczak, R. Hertel, M. Fähnle, H. Brückl, K. Rott, G. Reiss, I. Neudecker, D. Weiss, C. H. Back, and G. Schütz, Nature (London) **444**, 461 (2006).

[7]K. Yamada, S. Kasai, Y. Nakatani, K. Kobayashi, H. Kohno, A. Thiaville, and T. Ono, Nat. Mater. **6**, 270 (2007).

[8]R. P. Cowburn, Nat. Mater. **6**, 255 (2007).

[9]K. Yu. Guslienko, V. Novosad, Y. Otani, H. Shima, and K. Fukamichi, Phys. Rev. B **65**, 024414 (2001).

[10]S. Yakata, M. Miyata, S. Nonoguchi, H. Wada, and T. Kimura, Appl. Phys. Lett. **97**, 222503 (2010).

[11]N. Agarwal, D. J. Smith, and M. R. McCartney, J. Appl. Phys. **102**, 023911 (2007).

[12]K. Y. Guslienko, K. S. Lee, and S. K. Kim, Phys. Rev. Lett. **100**, 027203 (2008).

[13]M. Curcic, B. Van Waeyenberge, A. Vansteenkiste, M. Weigand, V. Sackmann, H. Stoll, M. Fähnle, T. Tyliszczak, G. Woltersdorf, C. H. Back, and G. Schütz, Phys. Rev. Lett. **101**, 197204 (2008).

[14]K. S. Lee, S.-K. Kim, Y.-S. Yu, Y.-S. Choi, K. Yu. Guslienko, H. Jung, and P. Fischer, Phys. Rev. Lett. **101**, 267206 (2008).

[15][http://math.nist.gov/oommf].

[16]A. Hubert and R. Schäfer, *Magnetic Domains: The Analysis of Magnetic Microstructures* (Springer, Berlin, 2008).

[17]H. F. Ding, A. K. Schmid, D. Li, K. Yu. Guslienko, and S. D. Bader, Phys. Rev. Lett. **94**, 157202 (2005).

[18]M. H. Park, Y. K. Hong, S. H. Gee, and D. W. Erickson, Appl. Phys. Lett. **83**, 329 (2003); H. Hu, H. Wang, M. R. McCartney, and D. J. Smith, Phys. Rev. B **73**, 153401 (2006); A. Lyle, Y.-K. Hong, B.-C. Choi, G. Abo, S. Bae, J. Jalli, J. Lee, M.-H. Park, and R. Syslo, J. Magn. **15**, 103 (2010).

[19]A. Kakay, Numerical Investigations of Micromagnetic Structures, Research Institute for Solid State Physics and Optics, Hungarian Academy of Sciences, Budapest, Hungary, 2005.

[20]K. Rivkin, K. Romanov, Y. Adamov, A. Abanov, V. Pokrovsky, and W. M. Saslow, Eur. Phys. Lett. **85**, 57006 (2009).